www.czasopisma.pan.pl PAN POLSKA AKADEMIA NAUK www.journals.pan.pl

A R C H I V E S O F M E T A L L U R G Y A N D M A T E R I A L S

Volume 56 2011 Issue 2

DOI: 10.2478/v10172-011-0030-z

E. RUDNIK*, J. SOBESTO*

CYCLIC VOLTAMMETRIC STUDIES OF TELLURIUM IN DILUTED HNO_3 SOLUTIONS

WOLTAMPEROMETRYCZNE BADANIA TELLURU W ROZCIEŃCZONYCH ROZTWORACH HNO_3

Electrochemistry of tellurium stationary electrode was studied in nitric acid solutions of pH 2.0 and 2.5. Two sparingly soluble products were formed at potentials above 200 mV (SCE): TeO_2 and H_2TeO_3. H_2TeO_3 and TeO_2 could dissolve to $HTeO_2^+$ under acidic electrolyte, but this process was hindered at pH 2.5. Cathodic polarization of tellurium electrode below –800 mV was accompanied by evolution of H_2Te, which was then oxidized at the potentials approx. –700 mV.

Keywords: tellurium; cyclic voltammetry; pH

Przeprowadzono elektrochemiczne badania zachowania się telluru w roztworach kwasu azotowego(V) o pH 2,0 i 2,5. Produktami utleniania telluru przy potencjałach powyżej 200 mV (wzgl. NEK) są słabo rozpuszczalne związki TeO_2 i H_2TeO_3. TeO_2 i H_2TeO_3 ulegają wtórnemu rozpuszczaniu w roztworze kwaśnym z utworzeniem $HTeO_2^+$, przy czym proces ten jest hamowany przy pH 2,5. W warunkach polaryzacji katodowej tellur metaliczny redukuje się do H_2Te (przy potencjałach poniżej –800 mV), który utlenia się przy potencjale ok. –700 mV.

1. Introduction

The electrochemistry of tellurium has been investigated intensively both in acidic [1, 2] and alkaline [2, 3] aqueous solutions. Recently, the studies have been focused on the electrodeposition of tellurium from Te(IV) acidic solutions [4-6] due to the increased interest in the electrochemical deposition of semiconductor thin layers [7-9]. However, there is relatively less information on the anodic oxidation of elemental tellurium. Awad [10] found that in acidic solutions ($HClO_4$, H_2SO_4, HNO_3) product of tellurium dissolution depend on the solution pH: soluble species ($HTeO_2^+$) form in the pH range of 0-0.8, H_2TeO_3 dominates at pH above 1.8, both compounds are present at intermediate pH, whereas Te_4^+ ions are produced at pH below 0. More extensive data were reported by Jayasekera et al. [11], who investigated both oxidation and reduction of tellurium in acidic and alkaline solutions. It was concluded that tellurous acid was mainly formed during tellurium oxidation followed by its slowly dissolution, whereas a type of product of tellurium electrochemical reduction was dependent on the solution pH.

The aim of presented work is to give additional insight into electrochemical processes occurring on the polycrystalline tellurium electrode in acidic solutions. This research work was a part of a larger project. It was undertaken in order to explain behavior of tellurium observed during industrial silver electrorefining in acidic nitrate solution. Anodic dissolution of doré metal enriched with tellurium led to the distribution of the impurity among the slime, electrolyte and cathodic deposit. The presence of tellurium ions in the bath had disadvantageous effect on the quality and purity of the cathodic silver [12, 13]. Transfer of tellurium from the anode to the electrolyte and then to the cathodic deposits was hindered by an increase in the solution pH in the range from 1.8 to 2.2 [14]. It led to accumulation of tellurium in the anodic slime, but a kind of tellurium compound in the slime remained undistinguished. Hence, the research was carried out to determine the anodic behavior of tellurium in nitrate solutions of two pH. The research will be continued to develop the mechanism of anodic dissolution of silver telluride Ag_2Te as a main form of tellurium in doré metal and obtained results will be reported later.

* AGH UNIVERSITY OF SCIENCE AND TECHNOLOGY, FACULTY OF NON-FERROUS METALS, DEPARTMENT OF PHYSICAL CHEMISTRY AND METALLURGY OF NON-FERROUS METALS LABORATORY OF PHYSICAL CHEMISTRY AND ELECTROCHEMISTRY, 30-059 KRAKÓW, 30 MICKIEWICZA AV., POLAND

2. Experimental

Electrochemical behavior of tellurium was studied in HNO_3 solutions at two pH: 2.0 and 2.5. Tellurium electrodes were prepared from polycrystalline tellurium pieces (99.9%). Surface active area of each electrode was approx. 1 cm^2. Prior to each experiment tellurium samples were polished with diamond slurry (with the grain gradation of 3μm and 1 μm). The electrodes were then thoroughly rinsed in deionized water and acetone. The stationary tellurium electrodes in non agitated baths (100 cm^3) were used. Each measurement was carried out with fresh tellurium surface and fresh electrolyte. Platinum plate (6 cm^2) was used as the counter electrode. The reference electrode was saturated calomel electrode (SCE) and all potentials are reported against this electrode. Electrochemical measurements were made using a potentiostat Atlas Sollich 98 EII. Tellurium electrode potentials were ranging from –1800 mV to 1300 mV (SCE) to cover all reactions of interest in the investigated system. The potential range was scanned in both positive-going and negative-going sweeps with various scan rates (1-100 mV/s). For detailed analysis, additional CV scans were registered in narrower potential ranges at a scan rate of 10 mV/s. Potentiostatic dissolution of tellurium was also carried out. Before and after potentiostatic measurement the electrode surface was observed by means of optical microscope, while EDS-SEM was used for chemical analysis of the solid products formed on tellurium. Concentration of tellurium species soluble in the electrolyte was determined by means of ICP method. All experiments were performed at room temperature.

3. Results and discussion

Fig. 1 shows CV curves for stationary tellurium electrode registered in nitrate solutions. Two anodic peaks (A_1, A_2) and two cathodic responses (C_1, C_2) were found in a potential range of –1800÷1300 mV (vs. SCE). The scanning of the potential from –1800 mV towards more positive values was accompanied initially by the flow of the cathodic current (C_2), but above –740 mV the anodic peak (A_2) appeared. Second anodic peak (A_1) was observed at potentials higher than 200 mV. In the reverse sweep, one cathodic peak (C_1) below –200 mV followed by the cathodic current flow (C_2) was appeared.

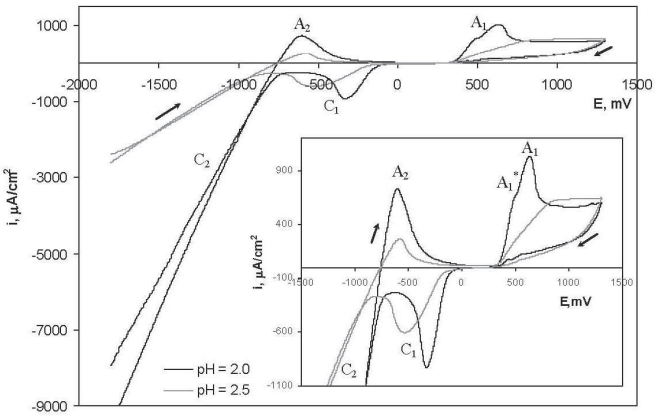

Fig. 1. Cyclic voltammograms for Te in HNO_3 solutions at pH 2.0 and 2.5. Scan rate: 10 mV/s; starting potential: –1800 mV (SCE); sweeps initiated towards positive potentials; switching reversal potential: 1300 mV(SCE)

Voltammograms show that relatively small increase in the solution pH affects seriously the rates of the electrochemical reactions indicated by decrease in current densities. It was especially visible in the potential range of C_2. Moreover, a change in the shape of the anodic peak A_1 was observed. In more acidic electrolyte evident peak A_1 with a maximum at 630 mV was accompanied by a kink A_1^* at the potential of approximately 480 mV in the forward scan. Two small corresponding peaks at the same potentials in the reverse scan were also found. At pH 2.5 only one wide anodic peak A_1 was developed in the voltammograms. It shows that two independent anodic reactions can occur at pH 2.0, but one of them is inhibited in less acidic solution. The cathodic peak C_1 was also reduced, when pH was increased. It became broader and its maximum displaced from –300 mV to approximately –500 mV. The height of the anodic peak A_2 decreased with the pH change from 2.0 to 2.5, but a peak maximum remained practically unchanged (approximately –670 mV).

Correlations between individual peaks were found in additional voltammetric measurements. They were performed in various potential ranges for each pH. Potential was cycled in four steps, but only two scans are presented in Fig. 2 for clarity, since no serious differences in the course of the curves were found. When potential sweep was commenced between 500 mV and –900 mV (Fig. 2 a, b), anodic currents above 300 mV (A_1) were accompanied by the cathodic peak (C_1) at the potentials of –200÷–250 mV followed by cathodic currents (C_2) below –750 mV. Anodic peak at –680 mV (A_2) emerged in the reverse sweep, but it was observed only at pH 2.0. If the potential sweep was extended to 800 mV or higher (Fig. 2c, d) evident oxidation peak A_1 (730±10 mV) was preceded by an additional anodic peak at approximately 500 mV (A_1^*) in more acidic solution, whereas only one

wide anodic peak (with a maximum at 740 mV) was developed at pH 2.5. Single cathodic peak C_1 was still visible in the negative-going sweeps. It shifted seriously towards more negative potentials from –220 mV at pH 2.0 to –390 mV at pH 2.5. The peak C_1 was not observed when sweeping was performed in the potential range of –200÷–700 mV (Fig. 2 e, f). It shows that the cathodic peak C_1 was due to the reduction of products of tellurium oxidation occurring at potentials above 300 mV.

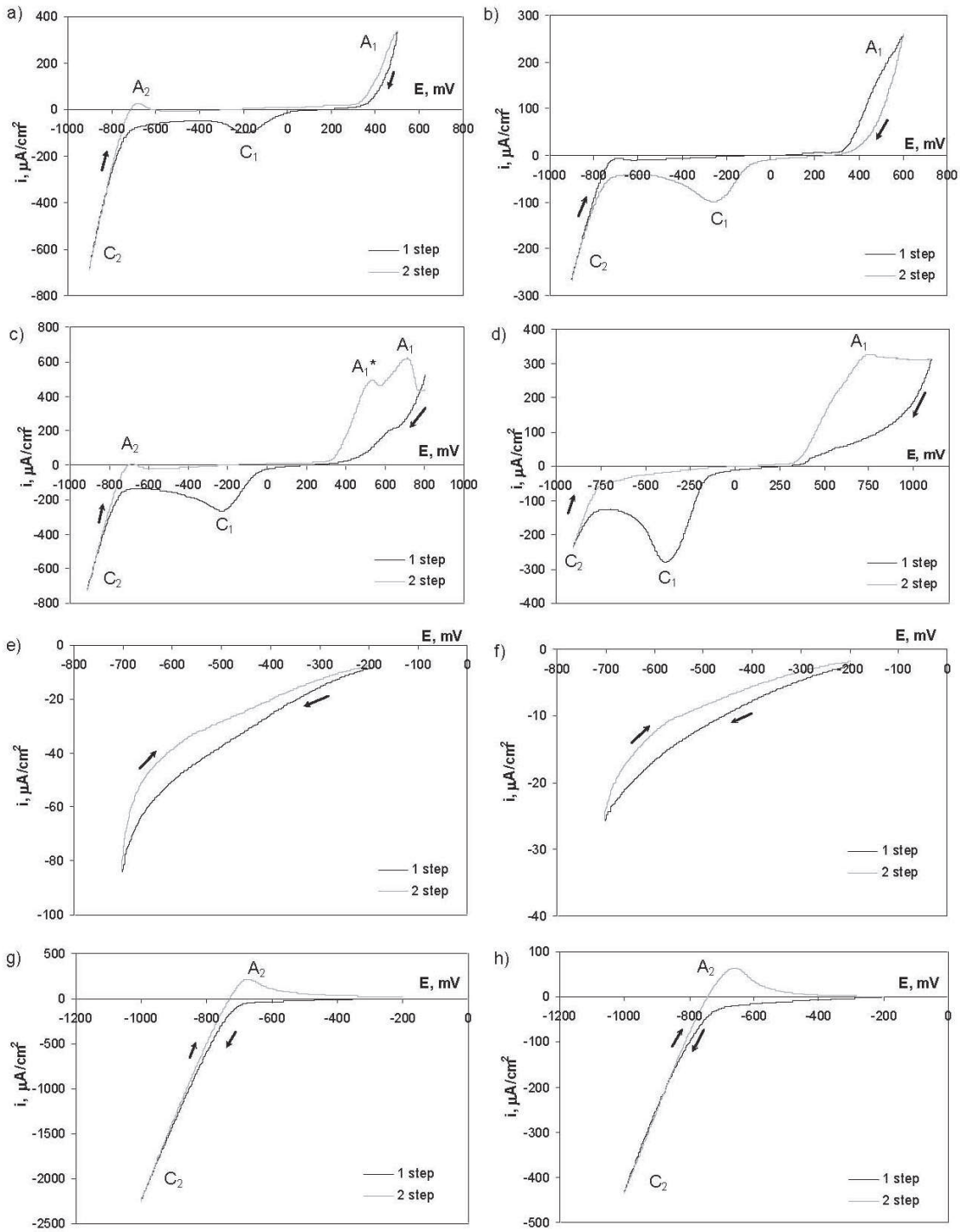

Fig. 2. Cyclic voltammograms for Te in HNO3 solutions of pH 2.0 (left side: a, c, e, g) and 2.5 (right side: b, d, f, h). Scan rate: 10 mV/s; sweeps initiated towards negative potentials

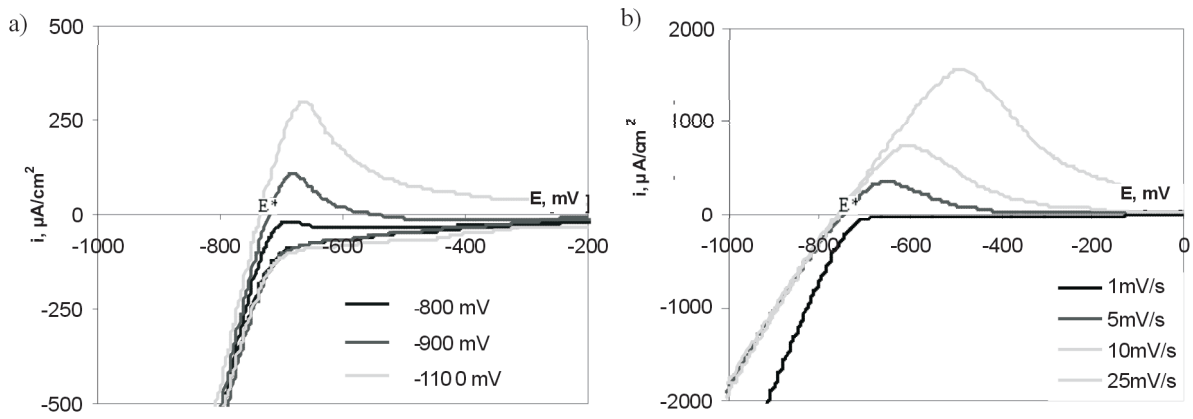

Fig. 3. Cyclic voltammograms registered for Te in HNO_3 solution of pH 2.0 from starting potential: –200 mV (SCE): a) scan rate: 10 mV/s, sweeps commenced towards negative direction to various switching potentials; b) various scan rates, sweeps commenced towards negative direction to –1800 mV

Cathodic polarization of tellurium electrode below –200 mV revealed that current flow in the range of –700÷–1000 mV (Fig. 2 g, h) gave the anodic peak A_2 at the potential of approximately –670 mV in the backward scan. This peak arose above the potential of approximately –730 mV (E^*) if the switching potential was shifted towards more negative values (Fig. 3a) or the sweep rate was increased (Fig. 3b), but it was significantly smaller at higher pH. It shows that a substrate oxidized during reverse scan was produced directly during preceding forward sweep at potentials below –800 mV.

Thermodynamic analysis was performed to elucidate the nature of the anodic and cathodic peaks. Table 1 summarizes standard and equilibrium potentials for tellurium electrodes calculated for two pH values. Obviously, position of the peaks on the potential axis can not correlate strictly to the equilibrium values due to overpotential necessary to drive the reactions. Tellurium can oxidize to three various products: soluble $HTeO_2^+$ ions and sparingly soluble TeO_2 and H_2TeO_3. It seems that the peak A_1 can be attributed undoubtedly to H_2TeO_3 formation, whereas $HTeO_2^+$ ions rather than TeO_2 can form at the peak A_1^*. However, the latter is not such evident. To verify the nature of the anodic peak A_1^* potentiostatic measurements were performed. Fig. 4 shows exemplary current-time plot registered at the potential of 480 mV. The transients were characterized by an initial decrease in current to a local maximum due to breakdown of the solid product layer. Finally, the steady-state current was achieved. Such a behavior was similar to current-time plots registered during anodic alumina formation [17]. According to mechanism of porous oxide layer growth the linear current fall corresponds to the formation of a planar oxide film, whereas a porous layer at the steady-state current is created. The shape of the curves seems to be a resultant of two overlapping processes – formation of the oxide layer and secondary dissolution of the solid product. It was supposed that initial dissolution of tellurium led to accumulate of $HTeO_2^+$ cations in the solution at the electrode surface and conditions for subsequent solid TeO_2 formation became thermodynamically possible.

TABLE 1

Electrode potentials (298 K)

Electrode reaction	Standard potential*, mV		Equilibrium potential**, mV (SCE)	
	vs. NHE	vs. SCE	pH = 2.0	pH = 2.5
$Te + 3H_2O \leftrightarrow H_2TeO_3 + 4H^+ + 4e$	614	373	255	225
$Te + 2H_2O \leftrightarrow HTeO_2^+ + 3H^+ + 4e$	550	309	147	124
$Te + 2H_2O \leftrightarrow TeO_2 + 4H^+ + 4e$	540	299	181	152
$2H_2Te_{aq} \leftrightarrow Te_2^{2-} + 4H^+ + 2e$	–142	–383	–471	–531
$H_2Te_{aq} \leftrightarrow Te + 2H^+ + 2e$	–471	–712	–683	–712
$Te_2^{2-} \leftrightarrow 2Te + 2e$	–800	–1041	–893	–893
$H_2 \leftrightarrow 2H^+ + 2e$	0	–241	–359	–389

*Standard electrode potentials were calculated according to standard free energies presented by Mc'Phail [15], except for $HTeO_2^+$ [16].

** Equilibrium potentials were calculated for 10^{-5} M tellurium soluble species.

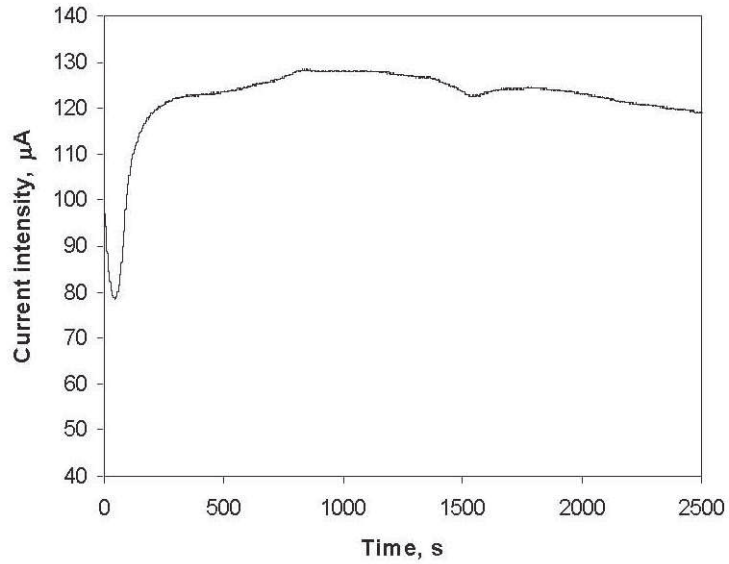

Fig. 4. Anodic current versus time for potentiostatic Te dissolution at potential of 480 mV (SCE) in HNO_3 solution of pH 2.0

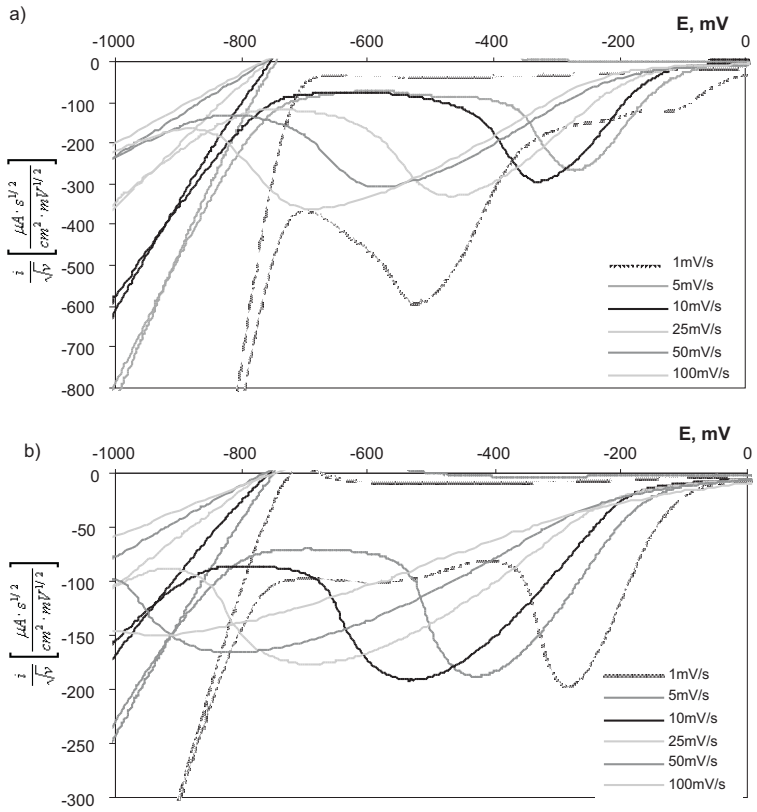

Fig. 5. Normalized cyclic voltammograms $i/v^{1/2} - E$ for Te in HNO_3 solutions for the cathodic peak C_1: a) pH = 2.0, b) pH = 2.5. Starting potential: 1300 mV (SCE), sweeps commenced towards negative direction to –1800 mV (SCE)

Growth of the oxide film was accompanied by its partial dissolution by the electrolyte. It was demonstrated in the voltammograms registered at various scan rates. Fig. 5 presents a part of data replotted as $i/v^{1/2}$ as a function of E for the peak C_1. Such voltammograms normalized the currents for the change in the rate of diffusion. Fig.5 shows changes characteristic for irreversible system, since increasing peak separation and reduction of the peak height with increased sweep rate were observed. However, one interesting feature for pH 2.0 but not for pH 2.5 was noticed in Fig. 5. At the lowest scan rate (1 mV/s) two cathodic peaks at approx. -150 mV and -500 mV were observed. It shows that tellurium oxide (or tellurous acid) dissolve partially to $HTeO_2^+$, which are then reduced at the potential -500 mV. At the lowest scan rate longer time was needed to sweep the potential from 1300 mV in the negative direction. It was sufficient to partial dissolution of oxide (or acid) film from the tellurium surface and to deliver a part of $HTeO_2^+$ ions from the electrode vicinity. Secondary dissolution of oxide (or acid) thin layer was prone in more acidic solution, since dissolution of tellurium oxide in acidic solution decreases with increased pH [18]. Reduction of solid products (TeO_2 or H_2TeO_3) occurred at higher potential (-200 mV).

Analysis of the electrolyte after potentiostatic dissolution was also carried out. It was found that mass of tellurium dissolved from the electrode at constant potential was less than theoretical value calculated using the Faraday's law. It confirmed that sparingly insoluble products form mainly on the electrode surface.

Potentiostatic oxidation of tellurium for a prolonged period of time (45 min) at 480 mV and 640 mV led to accumulation of solid products of the reactions on the electrode surface. Two kinds of products were observed by optical and scanning electron microscopes: octahedral crystals and a white amorphous layer. Fig. 6 shows the surface of tellurium after potentiostatic oxidation. EDS-SEM analysis of the crystals and white areas among the crystals showed the presence of tellurium and oxygen. The O:Te atomic ratio in the crystals was 1.52 (39.7 ± 0.4 at% Te, 60.3 ± 0.8 at% O) suggesting formation of TeO_2. Moreover, the shape of the crystals was suitable for tetragonal system of TeO_2 [16, 19]. The white product present on the electrode surface seemed to be porous and amorphous. It can correspond to tellurous acid H_2TeO_3 (TeO_2H_2O) [16]. It was difficult to determine definitely the formula of white compound due to simultaneous analysis of tellurium substrate.

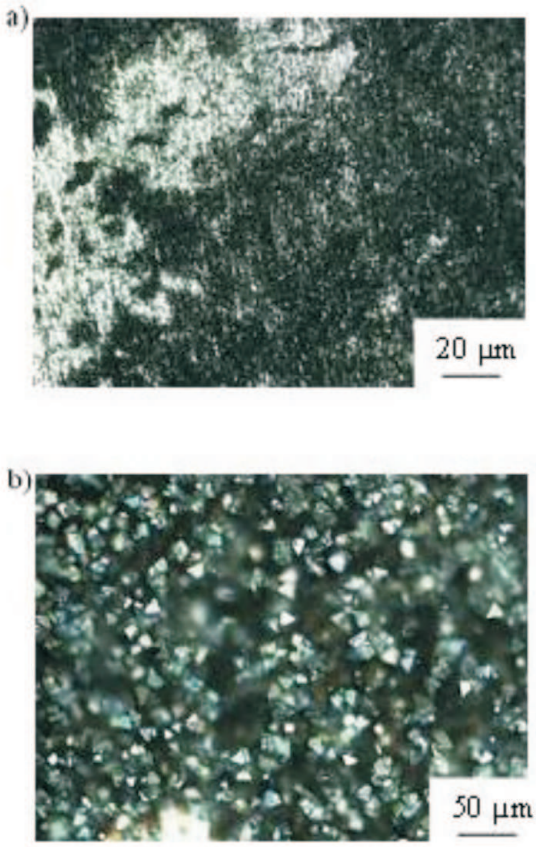

Fig. 6. Surface of tellurium after potentiostatic oxidation at 480 mV (SCE) in HNO_3 solution of pH 2.0

Reduction of tellurium at more negative potentials (less than -800 mV) caused changes on the electrode surface. It became dark at the potential of -1000 mV, but below -1100 mV a black slime run down into solution. The characteristic odor of hydrogen telluride H_2Te was also noticed during cathodic polarization. It shows that elemental tellurium reduces to H_2Te in the C_2 range. The gas was then reoxidized to tellurium during backward sweep at the potentials of the peak A_2. This was consistent with the thermodynamic predictions, since equilibrium potential for Te/H_2Te electrode at pH 2.0-2.5 was approximately -800 mV (Table 1).

Remaining electrochemical reactions presented in Table 1 were not taken into account, since no corresponding peaks in the voltammograms were found. However, coevolution of hydrogen at the potential range C_2 can not be excluded.

4. Conclusions

Electrochemistry of tellurium was studied in acidic nitrate solutions with pH 2.0 and 2.5. It was found that two sparingly soluble products were formed at potentials above 200 mV (SCE): TeO_2 and H_2TeO_3. The formation

of the solid products was almost undisturbed and no passivation was observed. H_2TeO_3 and TeO_2 can dissolve to $HTeO_2^+$ under acidic electrolyte, but this process was hindered by pH increase from 2.0 to 2.5. Cathodic polarization of tellurium electrode below -700 mV was accompanied by H_2Te evolution, which was then oxidized at the potentials approx. -700 mV (SCE).

Acknowledgements

This research study was financed from funds of Ministry of Science and Higher Education as a development project No. N R07 0017 04.

REFERENCES

[1] A.J. Bard (Ed), Encyclopaedia of electrochemistry of elements. **4**, Marcel Dekker, New York, 1975.
[2] Gmelin handbook of inorganic chemistry. Te., Suppl. **42**, 224-281 (1983).
[3] K.K. Mishra, D. Ham, K. Rajeshwar, Anodic oxidation of telluride ions in aqueous base: a rotating disc electrode study, J. Electrochem. Soc. **137(11)**, 3488-3441 (1990).
[4] J.M. Rosamilia, B. Miller, Voltammetric studies of tellurium film and hydrogen telluride formation in acidic tellurite solution, J. Electroanal. Chem. **215**, 261-271 (1986).
[5] E. Mori, C.K. Baker, J.R. Reynolds, K. Rajeshwar, Aqueous electrochemistry of tellurium at glassy carbon and gold. A combined voltammetry – oscillating quartz crystal microgravimetry study, J. Electroanal. Chem. **252**, 441-451 (1988).
[6] S. Dennison, S. Webster, An electrochemical and optical microscopic study of the reduction of $HTeO_2^+$ in aqueous acid solution, J.Electroanal.Chem. **314**, 207-222 (1991).
[7] B.W. Gregory, M.L. Norton, J.L. Stickney, Thin-layer electrochemical studies of the underpotential deposition of cadmium and tellurium on polycrystalline Au, Pt and Cu electrodes, J. Electroanal.Chem. **293**, 85-101 (1990).
[8] D-H. Han, S-J. Choi, S-M. Park, Electrochemical preparation of zinc telluride films on gold electrodes, J. Electrochem. Soc. **150** (5) C342-C346 (2003).
[9] M. S. Martin-Gonzalez, A. L. Prieto, R. Gronsky, T. Sands, A. M. Stacy, Insights into the electrodeposition of Bi_2Te_3, J. Electrochem. Soc. **149 (11)**, C546-C554 (2002).
[10] S.A. Awad, Anodic dissolution of tellurium in acid solutions, Electrochem. Acta. **12**, 925-936 (1968).
[11] S. Jayasekera, I.M. Ritchie, J. Avraamides, A cyclic voltammetric study of the dissolution of tellurium, Aust.J.Chem. **47(10)**, 1953-1965 (1994).
[12] N.D. Birjukov, A.V. Gulin, Investigation of the effect of various additives on cathodic deposition of silver in the presence of tellurium, Izv. SIB. OTD. Akad.Nauk. SSSR **4-9**, 20-24 (1969).
[13] P. Żabiński, L. Burzyńska, Influence of tellurium concentration on purity and morphology of cathodic silver, Rudy Metale **52 (2)**, 58-61 (2007).
[14] Effect of silver electrorefining parameters on tellurium content in silver cathode in the presence of tellurium-rich anodes, Report on a research work (No 5.5.180.336), AGH, Cracow, 2006.
[15] D.C. McPhail, Thermodynamic properties of aqueous tellurium species between 25 and 350°C, Geochim.Cosm. Acta **59(5)**, 851-866 (1995).
[16] M. Pourbaix, Atlas of Electrochemical Equilibria in Aqueus Solutions, Pergamon, New York, 1966.
[17] J. O'M. Bockris, R. E. White, B. E. Conwey (Eds.), Modern aspects of electrochemistry. No. 20, Plenum Press, New York, London.
[18] I.M. Issa, S.A. Awad, The amphoteric properties if tellurium dioxide, J. Phys. Chem. **58**, 948-951 (1954).
[19] A. Bielański, Podstawy chemii nieorganicznej, Wydawnictwo Naukowe PWN, Warszawa, 1994.

Received: 5 December 2010.